Treatment of Brain Tumors in Children Is Associated with Abnormal MR Spectroscopic Ratios in Brain Tissue Remote from the Tumor Site

Sandra M. Waldrop, Patricia C. Davis, Carol A. Padgett, Marla B. Shapiro, and Robin Morris

PURPOSE: Children who have brain tumors are at risk for a variety of treatment-related sequelae, including neuropsychological and cognitive impairment, neurologic deficits, and neuroendocrinologic disturbances. We sought to determine the value of proton MR spectroscopy in assessing brain tissue remote from the tumor site to ascertain the effects of chemotherapy and radiation treatment in these patients.

METHODS: Single-voxel proton MR spectra from 70 patients (111 spectra) and 11 healthy volunteers (11 spectra) were analyzed. NAA/Cr, NAA/Cho, and Cho/Cr ratios based on peak areas were obtained from nonneoplastic regions of the frontal lobe. The relationship between MR spectroscopic ratios and treatment was determined.

RESULTS: NAA-containing ratios were decreased in patients as compared with control subjects. The presence of gadolinium-based contrast material did not cause significant changes in the ratios as compared with precontrast data. When chemotherapy was a component of a child's treatment protocol, we found a significant decline in NAA/Cr ratios. Patients who underwent both chemotherapy and radiation therapy showed a trend toward lower NAA-containing ratios if the chemotherapy was administered before the radiation therapy. Patients receiving whole-brain radiation had a trend toward lower NAA-containing ratios than did those who had only focal tumor treatment.

CONCLUSION: In children with brain tumors, MR spectroscopy of brain tissue remote from the tumor reveals treatment-related biochemical changes.

Children who have brain tumors are at risk for a variety of treatment-related sequelae, including neuropsychological and cognitive impairment, neurologic deficits, and neuroendocrinologic disturbances (1–4). These may result from brain injury associated with the primary tumor itself, from surgical intervention, or from the effects of radiation therapy and chemotherapy on nontumorous brain tissue (5–8). Among the better-known adverse effects are those of radiation therapy, whether used alone or in combination with chemotherapy, with resultant leukoencephalopathy, vasculopathy, or tissue necrosis (8–15). The adverse effects of brain tumor treatment tend to worsen with time, with tumor relapse, and with multiple or aggressive therapies. Additionally, these effects are accentuated in children who are very young at the time of diagnosis (2).

While CT and MR imaging provide excellent anatomic information, there is a need for noninvasive physiological measurements that can serve as more sensitive markers for treatment-related effects on normal tissue. Proton MR spectroscopy provides biochemical information that can potentially affect treatment planning or prompt early intervention to prevent cognitive impairment.

MR spectroscopy uses MR technology to obtain additional information that is unavailable from anatomic MR imaging (16, 17). The signals typically studied with MR spectroscopy include moieties contain-

From the Department of Radiology, Emory University School of Medicine; the Department of Radiology, Egleston Children's Hospital at Emory University; and the Department of Psychology, Georgia State University, Atlanta.

Address reprint requests to Sandra M. Waldrop, PhD, Department of Radiology, Emory University Hospital, 1364 Clifton Rd, NE, Atlanta, GA 30322.
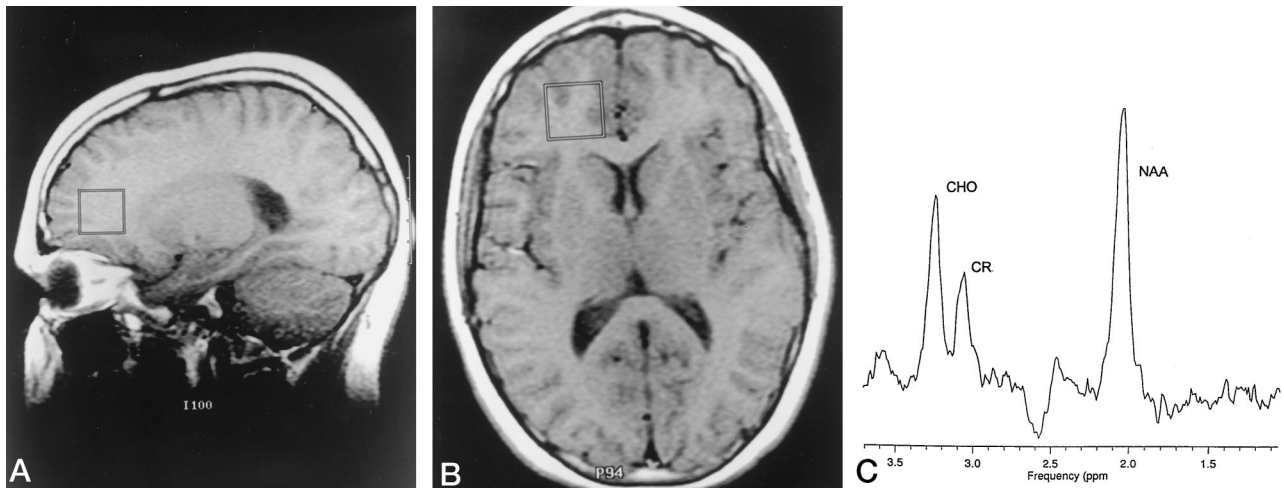
FIG 1.   MR images (2000/270) show voxel placement in sagittal (*A*) and axial (*B*) planes and on proton MR spectrum (*C*) (64 transients) in a healthy 11-year-old volunteer.

ing *N*-acetyl aspartate (NAA), a neuronal marker; choline (Cho), a marker of membrane integrity; creatine (Cr), a bioenergetic metabolite; and lactate, a marker of anaerobic metabolism (16, 17). Although experience to date is limited, other investigations have suggested a role for MR spectroscopy in the noninvasive assessment of tumor type and malignancy, tissue necrosis, ischemia, demyelination, and the effects of radiation therapy (18–26).

To investigate the role of MR spectroscopy as a marker for treatment-related effects, we successfully obtained 111 spectra from uninvolved brain tissue remote from the primary tumor site in 70 children with primary brain tumors, and 11 spectra from similar positions in 11 healthy pediatric volunteers. MR spectroscopic ratios (NAA/Cho, NAA/Cr, and Cho/Cr) were then compared with clinical parameters based on treatment protocols.

Methods

Subjects

MR spectroscopy was added to the clinically indicated MR imaging studies of 81 patients being followed up for primary brain neoplasms, resulting in 164 available spectra. Fifty-three MR spectroscopic examinations and 11 patients were excluded from further study owing to variable voxel placement early in our experience with MR spectroscopy, failure of automated MR spectroscopic shimming and water suppression, poor MR signal-to-noise ratio, or insufficient signal-to-noise and peak resolution for peak area measurements. Therefore, patient data from 111 MR spectra (70 patients, ages 2 to 22 years; mean age, 10.9 ± 5.0) and control data from 11 spectra (11 healthy volunteers, ages 7 to 15 years; mean age, 10.4 ± 2.9) are included in this report. In addition to these studies, comparison pre- and postcontrast spectra were obtained from the same frontal lobe location in 10 patients to establish the effect of paramagnetic contrast material on MR spectroscopic data. Informed consent as required by our institutional human investigation guidelines was obtained for all patients and volunteers. Children with braces, dental implants, preexisting neurologic or genetic conditions unrelated to tumor, insufficient sedation, or lack of cooperation for MR spectroscopic acquisition were excluded from the study.

MR Spectroscopic Data Acquisition and Processing

Spectra were acquired using the standard head coil on a 1.5-T system equipped with an automated program for single-voxel MR spectroscopic studies (PROBE/SV: GE Medical Systems; Milwaukee, WI). Single MR spectroscopic voxels (5 to 8 mm^3) containing a mixture of white and gray matter were located within the right or left frontal lobe remote from the tumor site at the level of the genu of the corpus callosum as determined from the midline sagittal scout image. Voxels were located graphically from an axial plane image (Fig 1). Spectra were acquired using a point-resolved spectroscopic (PRESS) sequence with parameters of 2000/270 (TR/TE), 64 or 128 acquisitions, 2048 data points, and a total examination time of 5 to 10 minutes per voxel. The gradient order was changed from the default order of *zxy* to *yxz* to compensate for inhomogeneities associated with voxel proximity to the paranasal sinuses (27). Baseline shimming of the magnet was performed approximately every 6 months to correct for excess automated shimming failures. Localized shimming of the voxel was performed before every examination.

Because paramagnetic contrast material was necessary for the neuroimaging portion of the study, the MR spectroscopic examinations in patients were completed within 25 minutes after administration of the contrast agent. Control subjects did not receive contrast material. Nineteen patients had additional spectra taken from the contralateral frontal lobe using identical MR spectroscopic parameters. Four patients had spectra from only the left frontal lobe owing to abnormalities in the right frontal lobe. To better determine the effect of paramagnetic contrast material on MR spectroscopic data, 10 patients had additional MR spectra taken before contrast administration.

MR spectroscopic data were processed on a workstation using Sage software (GE Medical Systems, Milwaukee, Wis), which included an automated sequence for the processing of PROBE data as described by Webb et al (28). The automated processing is designed to correct receiver-phase and phase errors due to eddy currents. The areas of spectral peaks representing NAA, Cho, and Cr were determined by digitizing the processed spectra. A baseline was estimated and the peaks were traced on a digitizing pad (Jandel Scientific Software, Chicago) interfaced to a computer running Sigma Scan (Jandel). NAA/Cr, NAA/Cho, and Cho/Cr ratios were calculated from these peak areas.

Because some patients were examined on multiple occasions during the course of this study, patients with repeat MR spectroscopic measurements without a change in treatment score were represented by an averaged value in the statistical calcu-

lations (n = 21 patients). Patients whose treatment score changed at the time of follow-up MR spectroscopy (n = 9) were represented more than one time in the statistical analysis that follows. Eight patients are represented by two scores each and one patient by three scores.

Clinical Data and Ratings

Chart review was completed for tumor type, age at diagnosis, tumor location, treatment history, clinical course, and MR imaging findings. Two experienced investigators who were blinded to the MR spectroscopic results assigned each child a consensus treatment score for each MR spectroscopic measurement, with points assigned as follows: presence of a tumor = 1, surgical resection = 1, radiation therapy = 1 per treatment course, and chemotherapy = 1 per treatment course. Control subjects received a score of zero. Because the treatment regimens encountered within this study varied considerably in dose and type of radiation therapy or chemotherapy, a detailed analysis of the effects of individual protocols of radiation therapy or chemotherapy was not attempted. Two items related to treatment protocol were examined for effects on MR spectroscopic ratios: the effect of whole-brain radiation versus focal tumor radiation therapy alone and the effect of order of administration of chemotherapy and radiation therapy. Chemotherapeutic agents represented in our patients' treatment regimens included vincristine, etoposide (VP-16), cyclophosphamide, cisplatin, ifosfamide, 5-fluorouracil, and carmustine. Radiation therapy courses were recorded by portal location as whole-brain and/or focal tumor therapy and by dose administered. Three children had only whole-brain treatment (4000 to 5400 cGy; mean, 4813 ± 727), 15 had only focal tumor portals (4500 to 5400 cGy; mean, 5109 ± 249) including one with an unknown dose, and 30 children had both whole-brain (2600 to 5040 cGy; mean, 3698 ± 589 cGy) and focal tumor (360 to 2400 cGy; mean, 1544 ± 494 cGy) therapy with a total dose of 4100 to 6720 cGy (mean, 5243 ± 526). Seven patients had radiation therapy at other institutions; thus, complete treatment details were not available.

Statistical Analysis

Statistical analyses were performed using SAS (SAS Institute, Cary, NC) and SPSS (SPSS, Inc, Chicago) statistical programs and included t-tests for independent and paired samples, Levene's test for equality of variances, one-way ANOVA, and Tukey analysis. The relationship was determined between MR spectroscopic ratios (NAA/Cho, NAA/Cr, and Cho/Cr) and the following: 1) left versus right frontal lobe voxel location; 2) presence or absence of paramagnetic contrast administration; 3) treatment score; 4) surgical resection, radiation therapy, or chemotherapy as components of a treatment protocol; 5) whole-brain radiation therapy (n = 3 whole brain and n = 30 whole brain plus focal tumor) versus focal tumor treatment alone; 6) relative order of chemotherapy and radiation therapy; and 7) tumor type. Probability levels of .05 were considered significant. Mean values are reported with standard deviations.

Results

The types of brain tumors found in the children in this study included primitive neuroectodermal tumor (PNET, n = 23), low-grade astrocytoma (n = 31), malignant astrocytoma or glioblastoma multiforme (n = 3), germ cell or germinoma (n = 4), craniopharyngioma (n = 2), ependymoma (n = 5), malignant melanoma (n = 1), and hemangiopericytoma (n = 1).

TABLE 1: Comparison of MR spectroscopic values obtained before and after administration of contrast material in 10 patients

Contrast Administration	NAA/Cr	NAA/Cho	Cho/Cr
Before	2.39 ± 0.22	1.82 ± 0.33	1.34 ± 0.25
After	2.60 ± 0.45	1.99 ± 0.15	1.31 ± 0.26

Left-Right Frontal Lobe MR Spectroscopic Comparisons

MR spectroscopic measurements were taken from both the right and left frontal lobe in 27 subjects (eight control subjects, 19 patients). None of the ratios had significant mean paired differences. The individual measurements for left versus right in a pair showed significant correlations for NAA/Cho ($P < .001$) and Cho/Cr ($P < .05$).

Effect of Contrast Material on MR Spectroscopic Ratios

A comparison of MR spectroscopic ratios obtained from matched voxels before and after administration of paramagnetic contrast agent is shown in Table 1. The effect of contrast material on the MR spectroscopic ratios was not significant.

Relationship between MR Spectroscopy and Brain Tumor Therapy

Examples of MR spectra for a control subject (rating of 0) and a patient with a treatment score of 5 are shown in Figures 1 and 2, respectively. Mean MR spectroscopic ratios for control subjects and patients are charted in Table 2. The NAA/Cho and NAA/Cr ratios are significantly decreased in patients versus control subjects. Patients subdivided by treatment score showed no statistically significant differences in MR spectroscopic ratios among groups; thus, no cumulative effect of multiple treatments was demonstrated. Treatment groups 1, 5, 6, and 7 were too small for statistical comparisons. Treatment group 4 was statistically different from the control group in the NAA/Cr ratio (Table 2).

Because most of the children were being treated with multiple regimens as part of a protocol, we attempted to dissect the synergistic effects of the combination of therapies (Table 3). MR spectroscopic ratios were grouped to show the effect of a particular treatment method within a treatment protocol, the effect of whole-brain radiation versus irradiation of only the tumor, and the effect of chemotherapy before radiation therapy.

Children who received chemotherapy as part of their overall treatment protocol had significantly lower NAA/Cr ratios than did patients not receiving chemotherapy (Table 3). The average age of the children receiving chemotherapy and radiation therapy was close to the average for the study, 10.9 years; thus, MR spectroscopic changes with age were not considered as factors in the MR spectroscopic data analysis (Table 3).
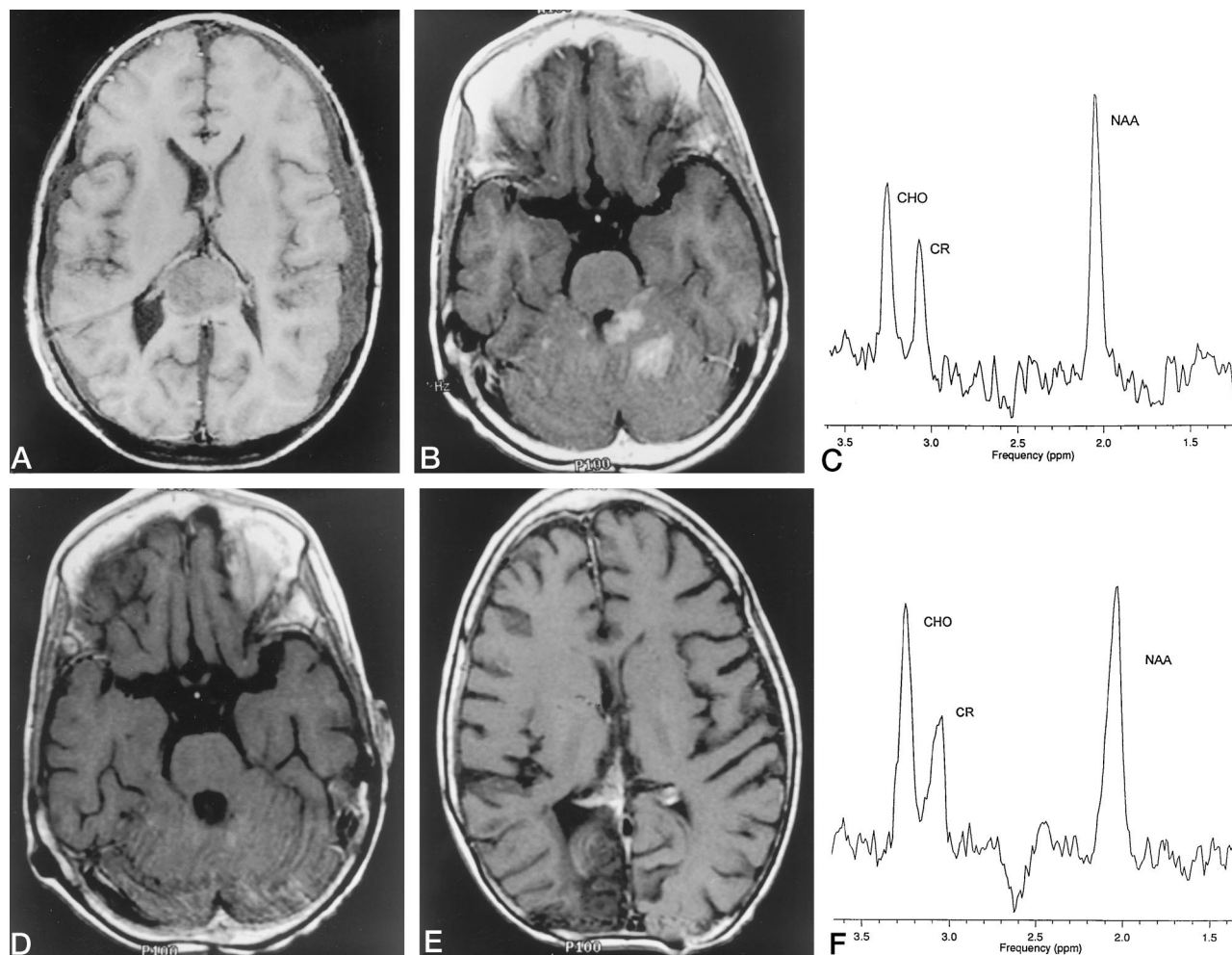
FIG 2.   MR study in 7-year-old boy with pineoblastoma (*A*) whose treatment included surgical debulking, chemotherapy, and cranio-spinal radiation. Five years later, the primary tumor recurred coincident with leptomeningeal dissemination (*B*). MR spectroscopy at that time (*C*) revealed the following ratios: NAA/Cho (1.70), NAA/Cr (2.42), and Cho/Cr (1.42). Although the patient responded to additional chemotherapy, with disappearance of MR evidence of leptomeningeal seeding and reduction in the size of the primary tumor (*D* and *E*), his MR spectrum (*F*) worsened, with a decrease in NAA/Cho (1.56) and NAA/Cr (2.11) ratios.

Children who received chemotherapy before radiation therapy had a trend toward lower NAA/Cr and NAA/Cho ratios than seen in children receiving radiation therapy only or radiation before chemotherapy (Table 3). Additionally, NAA/Cr and NAA/Cho ratios in the chemotherapy-first group were significantly lower ($P < .05$) than those of the control subjects.

As expected, ratios from children whose therapy included whole-brain radiation showed a trend toward lower NAA/Cr and NAA/Cho values as compared with children treated with focal tumor radiation therapy (Table 3). Children having whole-brain radiation therapy also had NAA/Cr and NAA/Cho ratios significantly lower than those of control subjects (Table 3). There was a significant linear relationship between whole-brain radiation dose and NAA/Cr ($r = -.67$, $P < .05$) in the 11 patients who did not have chemotherapy (Fig 3A). In patients who had both whole-brain radiation and chemotherapy (n = 22), there was no such linear trend ($r = .24$) (Fig 3B). Treatment via surgical resection had no significant effect on the ratios (Table 3).

Relationship between MR Spectroscopy and Tumor Type

A comparison of MR spectroscopic values by tumor type showed children with PNET to have NAA/Cr values significantly lower than those of control subjects ($P < .05$). Only the PNET, low-grade astrocytoma, and ependymoma groups were large enough for comparison (Table 4).

Discussion

Proton MR spectroscopy has proved helpful for studying brain tumor metabolism and for distinguishing tumor recurrence from radiation necrosis (21–24). Our study shows that single-voxel MR spectroscopy can be used successfully as an adjunct to MR imaging in the examination of treatment effects on uninvolved brain in children with primary brain tumors. In this study, MR spectroscopic ratios were obtained from a frontal lobe voxel that contained both white and gray matter. The voxel location was selected to include a substantial component of white matter, owing to the

TABLE 2: Mean MR spectroscopic ratios for all control subjects and treatment scores

	No.	NAA/Cr	NAA/Cho	Cho/Cr
Control subjects	11	2.77 ± 0.59	2.10 ± 0.43	1.34 ± 0.26
Patients	80	2.31 ± 0.47*	1.80 ± 0.37*	1.31 ± 0.25
Treatment score				
1	5	2.24 ± 0.37	1.70 ± 0.24	1.33 ± 0.26
2	24	2.43 ± 0.60	1.80 ± 0.36	1.36 ± 0.25
3	24	2.36 ± 0.48	1.83 ± 0.44	1.35 ± 0.30
4	18	2.13 ± 0.35†	1.75 ± 0.30	1.23 ± 0.18
5	6	2.28 ± 0.24	1.80 ± 0.39	1.29 ± 0.18
6	2	2.25 ± 0.25	2.07 ± 0.81	1.06 ± 0.20
7	1	2.55	1.88	1.36

* Ratios were significantly lower for all patients than for control subjects (*t*-test, $P < .05$).

† NAA/Cr ratios were significantly lower in these patients than in control subjects (Tukey analysis, $P < .05$).

TABLE 3: Effect of treatment methods on MR spectroscopic ratios

Treatment	No. of Patients	NAA/Cr	NAA/Cho	Cho/Cr
Chemotherapy				
No	48	2.42 ± 0.51	1.82 ± 0.35	1.36 ± 0.25
Yes	32	2.16 ± 0.35*	1.78 ± 0.41	1.25 ± 0.24
Chemotherapy only	4	2.12 ± 0.32	1.82 ± 0.31	1.18 ± 0.32
Chemotherapy then radiation therapy†	18	2.13 ± 0.34‡	1.65 ± 0.32‡	1.33 ± 0.25
Focal	2	2.33 ± 0.31	1.89 ± 0.41	1.24 ± 0.11
Whole, whole + focal	14	2.07 ± 0.32	1.59 ± 0.33	1.34 ± 0.27
Radiation therapy then chemotherapy†	10	2.28 ± 0.33	2.01 ± 0.44	1.14 ± 0.15
Focal	2	2.20 ± 0.37	2.19 ± 0.24	1.00 ± 0.06
Whole, whole + focal	7	2.23 ± 0.31	1.86 ± 0.42	1.20 ± 0.15
Radiation therapy				
No	26	2.35 ± 0.60	1.77 ± 0.34	1.33 ± 0.28
Yes†	54	2.30 ± 0.40	1.82 ± 0.39	1.30 ± 0.24
Focal	15	2.48 ± 0.45	1.98 ± 0.36	1.30 ± 0.29
Whole brain	33	2.19 ± 0.35‡	1.71 ± 0.37‡	1.31 ± 0.23
Surgical resection				
No	17	2.27 ± 0.41	1.74 ± 0.43	1.35 ± 0.28
Yes	63	2.33 ± 0.49	1.82 ± 0.36	1.30 ± 0.24

* All averaged treatment scores were significantly different (*t*-test, $P < .001$) when comparing the presence or absence of a treatment method.

† Details of radiation therapy portal and dose were not available for all children.

‡ Significantly different from control subjects (Tukey, $P < .05$).

known adverse effects of radiation and chemotherapy on white matter. Because we were studying a pediatric population, we expected a disproportionate number of primary tumors to be located in the posterior fossa. Our expectation was that treatment effects on nontumorous brain tissue could best be studied by using a voxel as anatomically distant from the primary tumor site as possible. Finally, since young children were included in the study, the larger size of the frontal lobe and ease of voxel positioning in younger children were advantageous. To offset the adverse effects of magnetic susceptibility artifacts from the paranasal sinuses on frontal lobe MR spectroscopic data, the gradient order was altered as described by Ernst and Chang (27).

The variability in left versus right frontal lobe MR spectroscopic ratios in this study was 20% (SD/mean × 100), well within the range of 18% to 38% variability that has been reported in other clinical MR spectroscopic studies (23, 37) and less than the frontal lobe variability recently reported by Jayasundar and Raghunathan (29). Although multisite automated single-voxel MR spectroscopic data from healthy adult volunteers have shown lower variability (10%) in MR spectroscopic ratios (28), to our knowledge this has not been achieved in patient studies. Factors affecting variability may include precision of voxel placement, magnetic susceptibility artifacts from the adjacent paranasal sinuses, subject motion, biological variation, and disease state (for patients). Our study indicates that owing to the variability of MR spectroscopic measurements, MR spectroscopic values are most useful as markers of treatment-related effects across a group of patients in whom multiple and longitudinal MR spectroscopic measurements are available. Single-patient or individual MR spectroscopic measurements should be used only with caution in conjunction with other clinical and imaging parameters as markers of treatment-associated effects in a given patient.

MR spectroscopic acquisitions using a long TE (270 milliseconds) were selected to maximize depiction of NAA, Cr, Cho, and lactate spectral peaks.

Brain tumor therapy has been associated with tissue changes resulting from ischemia, ischemic demyelination, and neuronal loss. Thus, we hoped that these would be apparent in the MR spectroscopic ratio changes.

Most studies of MR spectroscopy in tumor assessment use spectral data obtained from the same patient's nontumorous brain, contralateral or adjacent to the tumor site, for the normal comparison. Our study shows that there are measurable MR spectroscopic ratio differences in nontumorous brain tissue remote from the tumor site, possibly invalidating the assumption that spectra obtained from nontumorous brain parenchyma are "normal." Instead, it is likely that MR spectroscopic measurements from untreated brain that are acquired before tumor therapy treatment are more accurate for use as control or baseline values.

As expected, MR spectroscopic ratios from nontumorous brain tissue grouped by primary tumor type revealed few tumor-specific findings. The small size of many of the tumor groups prevented us from further analysis of this parameter.

Because we identified treatment-specific decreases in both NAA/Cho and NAA/Cr (Table 3) in the patient subgroups, our findings suggest that NAA is the major metabolite detectable by MR spectroscopy in nontumorous brain tissue affected by brain tumor therapy. Although NAA is considered to be a strong neuronal marker, its presence has been confirmed in
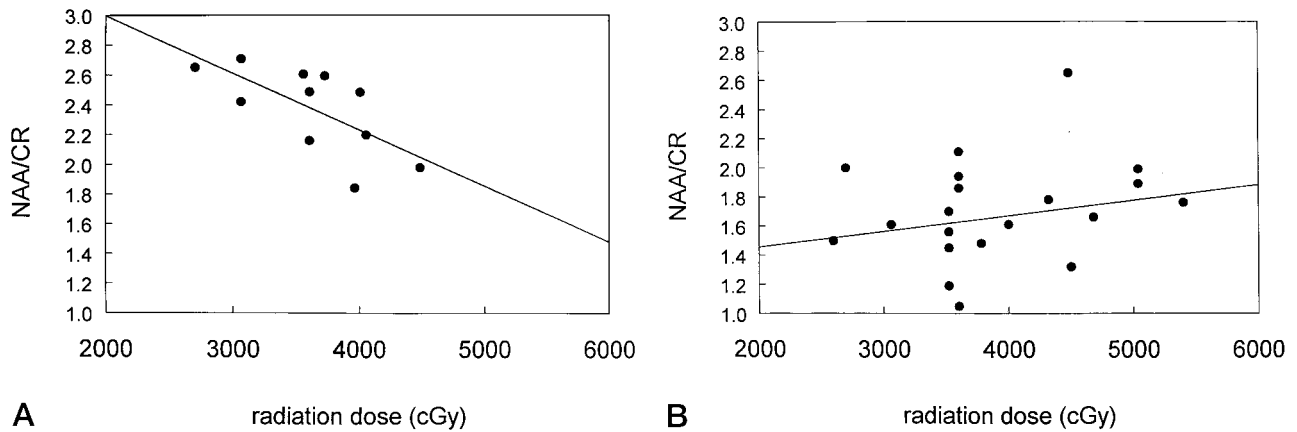
FIG 3.   Graphs show the relationship between NAA/Cr and whole-brain radiation in patients treated with radiation only ($r = -.67$, $P <$ .05, n = 11 patients) (*A*) and in those treated with radiation and chemotherapy ($r = .24$, n = 22 patients) (*B*).

TABLE 4: MR spectroscopic ratios for each tumor type

Tumor Type	No. of Patients	NAA/Cr	NAA/Cho	Cho/Cr
Control subjects	11	2.77 ± 0.59	2.10 ± 0.43	1.34 ± 0.26
Primitive neuroectodermal tumor	28	2.22 ± 0.36*	1.80 ± 0.44	1.29 ± 0.27
Low grade astrocytoma	33	2.43 ± 0.55	1.86 ± 0.32	1.32 ± 0.22
Malignant astrocytoma	3	2.22 ± 0.47	1.66 ± 0.46	1.38 ± 0.37
Ependymoma	8	2.08 ± 0.56	1.67 ± 0.41	1.24 ± 0.29
Germ cell	4	2.41 ± 0.32	1.80 ± 0.16	1.35 ± 0.19
Craniopharyngioma	2	2.50 ± 0.28	1.49 ± 0.17	1.68 ± 0.00
Other	2	2.30 ± 0.14	1.86 ± 0.25	1.25 ± 0.24

* NAA/Cr ratios were significantly lower in these patients than in control subjects (Tukey analysis, $P \leq .05$).

a variety of neural cells, within axons in both central and peripheral areas, and in nonneuronal as well as neuronal components in both white and gray matter (23, 30–32). Tedeschi et al (33) found larger NAA signals from the centrum semiovale than from cortical or thalamic gray matter, perhaps because of contributions from other *N*-acetyl compounds within myelinated tissue to the NAA spectral peak. In vitro identification of NAA was reported by Urenjak et al (32), with the unexpected finding of large amounts of NAA in oligodendrocyte type 2 astrocyte progenitor cells. Their data suggested that individual cell types showed characteristic patterns detectable by proton MR spectroscopy and that these patterns could aid in identifying tumor types.

NAA may play a variety of metabolic roles associated with neuronal protein synthesis, myelination, or brain neurotransmitter activity (30). A decrease in NAA has been linked to loss of neuronal activity in demyelinating disease that may precede detectable signal intensity changes on MR images (34). Reduced NAA has also been described in response to global hypoxic-ischemic injury that is poorly characterized by MR imaging in children who have nearly drowned (16). Thus, the decrease in NAA-containing ratios identified in our frontal lobe voxels could reflect subtle damage.

The Cr peaks in a spectrum are composed of creatine and phosphocreatine. Cr is about 20% higher in concentration in gray matter than in white matter, whereas in white matter, Cho peaks are only slightly higher than in gray matter (24, 31). Ross et al (24) found that the most apparent gray-white matter MR spectroscopic difference is the higher Cho/Cr ratio in gray matter, 0.83 versus 0.59 in white matter. Since in vivo MR spectroscopic studies are limited by use of relatively large voxels that include both gray and white matter, more studies may be needed to further clarify the contribution of Cr and Cho to MR spectroscopic ratios. Cr is reported to be diminished in hypoxia, stroke, tumor, and in young infants, but also varies in response to a variety of systemic metabolic states related to hepatic and renal metabolism (24).

The Cho peak that is detectable at MR spectroscopy is composed of glycerolphosphorylcholine, phosphorylcholine, and choline (24). Increases in Cho have been associated with disease conditions involving cellular destruction with loss of membrane and/or myelin integrity (24) and with brain tumors in which increased membrane synthesis and cellularity are present (35). Phosphatidylcholine in intact membranes and myelinated tissues probably does not contribute to the Cho MR spectroscopic signal (24). Elevated Cho and lactate have been described in areas of active demyelination, although the primary effect of demyelination is reflected in diminished NAA related to neuronal and axonal injury (24). Radiation effects include loss of NAA and increase in Cho (24).

Lactate is not generally detectable in normal brain tissue by MR spectroscopy when using a small voxel size and a minimum number of transients. Lactate peaks are visible in MR spectra of tumor cysts, necrotic tissues, secondary nonneuronal tumors, and in a variety of hypoxic events (24). Although it was anticipated that we would encounter MR spectroscopic evidence of lactate, the complete absence of lactate spectral peaks from nontumorous brain tissue in this study was not entirely surprising. Lactate clears rapidly from well-perfused tissue, such as nontumorous brain. Because our voxel position was intention-

ally selected to avoid proximity to a primary tumor site, tumor-associated lactate was avoided. None of the children in this study had clinical or radiologic evidence of overt or focal radiation necrosis; therefore, a lactate spectral peak related to radiation necrosis was not identified. Finally, although increased lactate has been described in the setting of acute and subacute cerebral infarction, none of the children experienced frontal lobe infarction either in association with radiation or other vascular disease in the area of voxel placement (36).

We anticipated at the outset that the primary MR spectroscopic relationship would reflect tissue ischemia and/or demyelination associated with radiation therapy and/or chemotherapy. Szigety et al (37) reported a comparative study of ^{31}P MR spectroscopy (13 patients) and proton MR spectroscopy (10 patients) in radiated nontumorous adult human brain tissue adjacent to a region of neoplasia and found no detectable differences in phosphorus in the radiated tissue. Proton spectroscopy, however, revealed metabolic abnormalities that were most noteworthy in brain regions that received the highest doses of radiation. Because both Cr/Cho and NAA/Cho ratios decreased after radiation therapy, these authors postulated that the primary effect on radiated nontumorous brain tissue was a release of membrane-bound Cho related to membrane lipid breakdown at a cellular level, although it was recognized that a decrease in NAA could be contributory to the alterations in the MR spectroscopic ratio. In another study of radiation effects on nontumorous brain tissue, Usenius et al (38) reported quantitative proton MR spectroscopic findings from tissue adjacent to tumor sites in eight adults who had undergone radiation therapy. By using brain water concentration as an internal reference, these investigators found it apparent that the primary metabolic abnormality was a decrease in NAA, with relative stability of Cho and Cr values. Furthermore, Yousem et al (25) reported a reduction in NAA/Cho and NAA/Cr in brains of irradiated cats from tissue that was normal in intensity at MR imaging. The voxel position in our study was more remote from primary tumor sites than in the above studies and the brain tissue evaluated was more normal in intensity at MR imaging. The fact that the MR spectroscopic findings of declining NAA-containing ratios were greater for whole-brain radiation than for irradiation of the tumor only (Table 3) in our study suggests that radiation therapy, although not the sole explanation, may contribute to the MR spectroscopic ratio changes found in our population.

We found significantly lower NAA/Cr ratios in children who received chemotherapy as part of their treatment than in those who did not. Although most of the patients receiving chemotherapy also received radiation, patients administered chemotherapy before radiation therapy had a trend toward lower NAA/Cr and NAA/Cho (in particular), which may reflect synergistic or sensitizing effects of some chemotherapeutic agents. Moreover, although the group is small, those patients receiving only chemotherapy

also had reduced NAA/Cr ratios without the lowering in NAA/Cho seen with radiation. The modulating effect of chemotherapy can also be appreciated by comparing NAA/Cr values with radiation dose. When chemotherapy was absent, there was a linear decrease in NAA/Cr with increasing dose (Fig 3A). When chemotherapy was present, the NAA/Cr values were decreased without regard to radiation dose (Fig 3B).

In this study, the MR spectroscopic data were acquired after all clinically relevant imaging sequences were completed. As a result, all patient MR spectroscopic data were acquired after administration of a paramagnetic contrast agent. While we would have preferred to acquire the MR spectroscopic data before contrast administration, doing so might have jeopardized the ability to complete the clinical study without the use of additional sedation. And although contrast material might affect MR spectroscopic ratios from tumor sites, our comparison of pre- and postcontrast patient data did not show a significant difference in MR spectroscopic ratios from nontumorous brain voxels.

For future investigations of associated effects of tumor treatment, the techniques of short-echo single-voxel MR spectroscopy and chemical shift imaging (CSI) appear promising. Short-echo MR spectroscopic studies offer a way to map more cerebral metabolites, such as amino acids, that may be more sensitive markers for the effects of brain tumor therapy. CSI offers a comparative analysis of metabolite peaks or metabolite mapping across a relatively large tissue volume (39). CSI techniques thus could be used to confirm single-voxel findings as treatment-associated effects. With further experience and larger patient populations, more subtle effects of individual treatment regimens and the relationship between treatment, MR spectroscopic findings, and clinical and neuropsychological effects could be elucidated.

Conclusions

Our findings indicate that the effects of brain tumor therapy are associated with measurable changes in NAA/Cho and NAA/Cr ratios from nontumorous brain tissue in children with primary brain neoplasms as compared with healthy children. The most consistent finding was a decrease in NAA/Cr. Chemotherapy as one component of a multitreatment protocol was associated with significant reduction in the NAA/Cr ratio. There was a trend for patients treated with chemotherapy before radiation therapy to have lower NAA/Cr and NAA/Cho ratios, suggesting that chemotherapy may alter the subsequent biochemical effects of radiation therapy. Although we anticipated a strong relationship between the MR spectroscopic ratios and the use of radiation therapy, we instead found a trend toward lower NAA/Cr and NAA/Cho ratios in children treated with whole-brain radiation relative to those treated only with focal tumor therapy and to those not treated with radiation therapy. Although further experience is needed, our study suggests a potential role for MR spectroscopy in moni-

toring the effects of treatment on nontumorous brain tissue.

References

1. Duffner PK, Cohen ME, Parker MS. **Prospective intellectual testing in children with brain tumors.** *Ann Neurol* 1988;23:575–579
2. Packer RJ, Sutton LN, Atkins TE, et al. **A prospective study of cognitive function in children receiving whole-brain radiotherapy and chemotherapy: 2-year results.** *J Neurosurg* 1989;70:707–713
3. Ellenberg L, McComb JG, Siegel SE, Stowe S. **Factors affecting intellectual outcome in pediatric brain tumor patients.** *Neurosurgery* 1987;21:638–644
4. Constine LS, Woolf PD, Cann D, et al. **Hypothalamic-pituitary dysfunction in radiation for brain tumors.** *N Engl J Med* 1993;328:87–94
5. Syndikus I, Tait D, Ashley S, Jannoun L. **Long-term follow-up of young children with brain tumors after irradiation.** *Int J Radiat Oncol Biol Phys* 1994;30:781–787
6. DeAngelis LM, Shapiro, WR. **Drug/radiation interactions and the central nervous system.** In: Gutin PH, Leibel SA, Sheline GE, eds. *Radiation Injury to the Nervous System.* New York: Raven Press; 1991:361–382
7. Wang G-J, Volkow ND, Lau YH, et al. **Glucose metabolic changes in nontumoral brain tissue of patients with brain tumor following radiotherapy: a preliminary study.** *J Comput Assist Tomogr* 1996;20:709–714
8. Davis PC, Hoffman JC, Pearl GS, Braun IF. **CT evaluation of effects of cranial radiation therapy in children.** *AJNR Am J Neuroradiol* 1986;7:639–644
9. Valk PE, Dillon WP. **Radiation injury of the brain.** *AJNR Am J Neuroradiol* 1991;12:45–62
10. Hopewell JJWJ. **The importance of vascular damage in the development of late radiation effects in normal tissues.** In: Meyn RE, Withers HR, eds. *Radiation Biology in Cancer Research.* New York: Raven Press; 1980:449–459
11. Dooms GC, Hecht S, Brant-Zawadzki M, Berthiaume Y, Norman K, Newton TH. **Brain radiation lesions: MR imaging.** *Radiology* 1986;158:149–155
12. Poussaint TY, Siffert J, Barnes PD, et al. **Hemorrhagic vasculopathy after treatment of central nervous system neoplasia in childhood: diagnosis and follow-up.** *AJNR Am J Neuroradiol* 1995;16:693–699
13. Gaensler EHL, Dillon WP, Edwards MSB, Larson DA, Rosenau W, Wilson CB. **Radiation-induced telangiectasia in the brain simulates cryptic vascular malformations at MR imaging.** *Radiology* 1994;193:629–636
14. Tsuruda JS, Kortman KE, Bradley WG, Wheeler DC, Van Dalsem W, Bradley TP. **Radiation effects on cerebral white matter: MR evaluation.** *AJNR Am J Neuroradiol* 1987;8:431–437
15. Wright TL, Bresnan MJ. **Radiation-induced cerebrovascular disease in children.** *Neurology* 1976;26:540–543
16. Moats RA, Watson L, Shonk T, et al. **Added value of automated clinical proton MR spectroscopy of the brain.** *J Comput Assist Tomogr* 1995;19:480–491
17. Wang Z, Zimmerman RA, Sauter R. **Proton MR spectroscopy of the brain: Clinically useful information obtained in assessing CNS diseases in children.** *AJR Am J Roentgenol* 1996;167:191–199
18. Sutton LN, Wehrli SL, Gennarelli L, et al. **High-resolution ^{1}H-magnetic resonance spectroscopy of pediatric posterior fossa tumors in vitro.** *J Neurosurg* 1994;81:443–448
19. Tzika AA, Dunn RS, Webb P, Kohler SJ, Raidy T, Hurd R. **Evaluation of the clinical performance of automated proton magnetic spectroscopy in children.** *Acad Radiol* 1994;1:46–50
20. Tzika AA, Vigneron DB, Ball WS, Dunn RS, Kirks DR. **Localized proton MR spectroscopy of the brain in children.** *J Magn Reson Imaging* 1993;3:719–729
21. Tzika AA, Vigneron DB, Dunn RS, Nelson SJ, Ball WS Jr. **Intracranial tumors in children: small single-voxel proton MR spectroscopy using short- and long-echo sequences.** *Neuroradiology* 1996;38:254–263
22. Negendank WG, Sauter R, Brown TR, et al. **Proton magnetic resonance spectroscopy in patients with glial tumors: a multicenter study.** *J Neurosurg* 1996;84:449–458
23. Tien RD, Lai PH, Smith JS, Lazeyras F. **Single-voxel proton brain spectroscopy exam (PROBE/SV) in patients with primary brain tumors.** *AJR Am J Roentgenol* 1996;167:201–209
24. Ross BD, Michaelis T. **Clinical applications of magnetic resonance spectroscopy.** *Magn Reson Q* 1994;10:191–247
25. Yousem DM, Lenkinski RE, Evans S, et al. **Proton MR spectroscopy of experimental radiation-induced white matter injury.** *J Comput Assist Tomogr* 1992;16:543–548
26. Grossman RI, Hecht-Leavitt CM, Evans SM, et al. **Experimental radiation injury: combined MR imaging and spectroscopy.** *Radiology* 1988;169:305–309
27. Ernst T, Chang L. **Elimination of artifacts in short echo time ^{1}H MR spectroscopy of the frontal lobe.** *Magn Reson Med* 1996;36:462–468
28. Webb PG, Sailasuta N, Kohler SJ, Raidy T, Moats RA, Hurd RE. **Automated single-voxel proton MRS: technical development and multisite verification.** *Magn Reson Med* 1994;31:365–373
29. Jayasundar R, Raghunathan P. **Evidence for left-right asymmetries in the proton MRS of brain in normal volunteers.** *Magn Reson Med* 1997;15:223–234
30. Birken DL, Oldendorf WH. **N-Acetyl-L-aspartic acid: a literature review of a compound prominent in ^{1}H-NMR spectroscopic studies of brain.** *Neurosci Behav Rev* 1989;13:23–31
31. Hetherington HP, Mason GF, Pan JW, et al. **Evaluation of cerebral gray and white matter metabolite differences by spectroscopic imaging at 4.1T.** *Magn Reson Med* 1994;32:565–571
32. Urenjak J, Williams SR, Gadian DG, Noble M. **Proton nuclear magnetic resonance spectroscopy unambiguously identifies different neural cell types.** *J Neurosci* 1993;13:981–989
33. Tedeschi G, Righini A, Bizzi A, Barnett AS, Alger JR. **Cerebral white matter in the centrum semiovale exhibits a larger N-acetyl signal than does gray matter in long echo time ^{1}H-magnetic resonance spectroscopic imaging.** *Magn Reson Med* 1995;33:127–133
34. Rajanayagam V, Grad J, Krivit W, et al. **Proton MR spectroscopy of childhood adrenoleukodystrophy.** *AJNR Am J Neuroradiol* 1996;17:1013–1024
35. Fulham MJ, Bizzi A, Dietz MJ, et al. **Mapping brain tumor metabolites with proton MR spectroscopic imaging: clinical relevance.** *Radiology* 1992;185:675–686
36. Mathews VP, Barker PB, Blackband SJ, Chatham JC, Bryan RN. **Cerebral metabolites in patients with acute and subacute strokes: concentrations determined by quantitative proton MR spectroscopy.** *AJR Am J Roentgenol* 1995;165:633–638
37. Szigety SK, Allen PS, Huyser-Wierenga D, Urtasun RC. **The effect of radiation on normal human CNS as detected by NMR spectroscopy.** *Int J Radiat Oncol Biol Phys* 1993;25:695–701
38. Usenius T, Usenius JP, Tenhunen M, et al. **Radiation-induced changes in human brain metabolites as studied by ^{1}H nuclear magnetic resonance spectroscopy in vivo.** *Int J Radiat Oncol Biol Phys* 1995;33:719–724
39. Leach MO. **Practicalities of localization in animal and human tumours.** *NMR Biomed* 1992;5:244–252